

Low-lying excitations in ^{72}Ni

A. I. Morales,^{1,2,*} G. Benzoni,² H. Watanabe,^{3,4} S. Nishimura,³ F. Browne,^{5,3} R. Daido,⁶ P. Doornenbal,³ Y. Fang,⁶ G. Lorusso,³ Z. Patel,^{7,3} S. Rice,^{7,3} L. Sinclair,^{8,3} P.-A. Söderström,³ T. Sumikama,⁹ J. Wu,³ Z. Y. Xu,^{10,3} A. Yagi,⁶ R. Yokoyama,¹¹ H. Baba,³ R. Avigo,^{1,2} F. L. Bello Garrote,¹² N. Blasi,² A. Bracco,^{1,2} F. Camera,^{1,2} S. Ceruti,^{1,2} F. C. L. Crespi,^{1,2} G. de Angelis,¹³ M.-C. Delattre,¹⁴ Zs. Dombradi,¹⁵ A. Gottardo,¹³ T. Isobe,³ I. Kojouharov,¹⁶ N. Kurz,¹⁶ I. Kuti,¹⁵ K. Matsui,¹⁰ B. Melon,¹⁷ D. Mengoni,^{18,19} T. Miyazaki,¹⁰ V. Modamio-Hoyborg,¹³ S. Momiyama,¹⁰ D. R. Napoli,¹³ M. Niikura,¹⁰ R. Orlandi,^{20,21} H. Sakurai,^{3,10} E. Sahin,¹² D. Sohler,¹⁵ H. Shaffner,¹⁶ R. Taniuchi,¹⁰ J. Taprogge,^{22,23} Zs. Vajta,¹⁵ J. J. Valiente-Dobón,¹³ O. Wieland,² and M. Yalcinkaya²⁴

¹*Dipartimento di Fisica dell'Università degli Studi di Milano, I-20133 Milano, Italy*

²*Istituto Nazionale di Fisica Nucleare, Sezione di Milano, I-20133 Milano, Italy*

³*RIKEN Nishina Center, 2-1 Hirosawa, Wako, Saitama 351-0198, Japan*

⁴*IRCNPC, School of Physics and Nuclear Engineering, Beihang University, Beijing 100191, China*

⁵*School of Computing, Engineering, and Mathematics, University of Brighton, Brighton, United Kingdom*

⁶*Department of Physics, Osaka University, Osaka 560-0043 Toyonaka, Japan*

⁷*Department of Physics, University of Surrey, Guildford GU2 7XH, United Kingdom*

⁸*Department of Physics, University of York, Heslington, York YO10 5DD, United Kingdom*

⁹*Department of Physics, Tohoku University, Miyagi 980-8578, Japan*

¹⁰*Department of Physics, University of Tokyo, Hongo7-3-1, Bunkyo-ku, 113-0033 Tokyo, Japan*

¹¹*CNS, University of Tokyo, Tokyo 351-0198, Japan*

¹²*Department of Physics, University of Oslo, N-0316 Oslo, Norway*

¹³*Istituto Nazionale di Fisica Nucleare, Laboratori Nazionali di Legnaro, I-35020 Legnaro, Italy*

¹⁴*IPNO Orsay, 91400 Orsay, France*

¹⁵*MTA Atomki, H-4001 Debrecen, Hungary*

¹⁶*GSI, Planckstrasse 1, D-64291 Darmstadt, Germany*

¹⁷*INFN Sezione di Firenze, I-50019 Firenze, Italy*

¹⁸*Dipartimento di Fisica dell'Università degli Studi di Padova, I-35131 Padova, Italy*

¹⁹*Istituto Nazionale di Fisica Nucleare, Sezione di Padova, I-35131 Padova, Italy*

²⁰*Instituut voor Kern- en StralingsFysica, K.U. Leuven, B-3001 Heverlee, Belgium*

²¹*Advanced Science Research Center, JAEA, Tokai, Ibaraki 319-1195, Japan*

²²*Instituto de Estructura de la Materia, CSIC, E-28006 Madrid, Spain*

²³*Departamento de Física teórica, Universidad Autónoma de Madrid, E-28049 Madrid, Spain*

²⁴*Department of Physics, Istanbul University, 34134 Istanbul, Turkey*

(Received 11 November 2015; revised manuscript received 26 January 2016; published 22 March 2016)

Low-lying excited states in ^{72}Ni have been investigated in an in-flight fission experiment at the RIBF facility of the RIKEN Nishina Center. The combination of the state-of-the-art BigRIPS and EURICA setups has allowed for a very accurate study of the β decay from ^{72}Co to ^{72}Ni , and has provided first experimental information on the decay sequence $^{72}\text{Fe} \rightarrow ^{72}\text{Co} \rightarrow ^{72}\text{Ni}$ and on the delayed neutron-emission branch $^{73}\text{Co} \rightarrow ^{72}\text{Ni}$. Accordingly, we report nearly 60 previously unobserved γ transitions which deexcite 21 new levels in ^{72}Ni . Evidence for the location of the so-sought-after (4_2^+) , (6_2^+) , and (8_1^+) seniority states is provided. As well, the existence of a low-spin β -decaying isomer in odd-odd neutron-rich Co isotopes is confirmed for mass $A = 72$. The new experimental information is compared to simple shell-model calculations including only neutron excitations across the fpg shells. It is shown that, in general, the calculations reproduce well the observed states.

DOI: [10.1103/PhysRevC.93.034328](https://doi.org/10.1103/PhysRevC.93.034328)

I. INTRODUCTION

The semimagic isotopic chain of Ni ($Z = 28$), spanning three nuclear neutron-shell closures ($N = 20, 28$, and 50) and a presumable $N = 40$ harmonic-oscillator shell gap, represents an excellent testing ground for forefront theoretical calculations aiming at describing the evolution of nuclear structure

from stability to remote unstable regions [1–5]. Experimental constraints in this isotopic chain may help to better understand the role played by different components of the nuclear force in driving shell evolution and deformation. Sensitive probes for this are the Ni nuclei between $N = 40$ and 50 , in which near-spherical configurations typical of semimagic nuclei are predicted to coexist with low-lying intruder configurations stabilized by the tensor force of the proton-neutron monopole interaction [1,2]. This shape coexistence phenomenon is most likely induced by both proton and neutron excitations within the same system [2]: The promotion of neutrons from the lower

*Also at IFIC, CSIC-Universitat de València, València, Spain; Ana.Morales@ific.uv.es

subshells to the $g_{9/2}$ orbital at increasing excitation energy results in a reduction of the energy gap between the proton spin-orbit partners $f_{7/2}$ - $f_{5/2}$ through the monopole tensor force. This reduction facilitates the excitation of proton pairs across the $Z = 28$ shell closure. A larger occupation of the $f_{5/2}$ proton orbit simultaneously lowers the $g_{9/2}$ neutron subshell and therefore enhances further neutron particle-hole excitation across the $N = 40$ subshell closure. Accordingly, low-lying strongly deformed bands, stable against the spherical shape, are expected to appear in the neutron-rich Ni isotopes [2]. Nonyrast 0^+ and 2^+ states observed at relatively low excitation energies in ^{68}Ni and ^{70}Ni were interpreted as being ascribed to the deformed structures [6–11]. The next even-even isotope, ^{72}Ni , might be at the core of the region of shape coexistence in the Ni chain: At variance with some state-of-the-art shell-model approaches [4], recent Monte Carlo shell-model calculations [2] predict a deep prolate minimum in ^{72}Ni at the lowest excitation energy among the Ni isotopes. Experimental information on the low-lying structure of this nucleus, hence, may help to benchmark the latest shell-model interactions.

The Ni nuclei have also attracted attention owing to the absence of μs -seniority isomers in ^{72}Ni and ^{74}Ni [12,13]. The seniority ν , which indicates the number of nucleons that are not in pairs coupled to angular momentum $J = 0$, has shown to be a good quantum number for semimagic nuclei along the whole nuclear chart [14]. Many properties of these nuclei can be described well within the seniority scheme [15] as the constancy of energies for states of equal seniority, which are independent of the number of nucleons filling the shell, and the hindrance of transitions generated by quadrupole operators between states of equal seniority, which is maximum when the orbital is half filled. Accordingly, the isomerism in the fully aligned members of the $\nu = 2$ configuration results from a combination of a small energy spacing with respect to the next lower-lying $\nu = 2$ level and the seniority cancellation near the middle of the valence shell. The observation of a 232(1)-ns 8^+ isomer in ^{70}Ni [16] raised expectations for the seniority scheme to describe satisfactorily the nuclear structure of the semimagic Ni isotopes with neutrons filling the $\nu g_{9/2}$ shell. Seniority long-lived 8^+ states have also been reported for the valence mirror symmetry $N = 50$ isotones [17] and the neutron-rich Cd and Pd isotopes with $N = 82$ [18,19], where protons occupy the $0g_{9/2}$ orbital, and for the heavy neutron-rich Pb isotopes where neutrons occupy the $1g_{9/2}$ shell [20]. However, in the Ni isotopic chain, the 8^+ isomer is found again only in ^{76}Ni , with a reported half-life of $t_{1/2} = 547.8(33)$ ns [21]. The first theoretical explanation for the disappearance of the midshell seniority isomerism came from Grawe *et al.* [22], and was later supported by Lisetskyi *et al.* [23] and Van Isacker [24]. In ^{72}Ni and ^{74}Ni , with four neutrons and four neutron holes occupying the $0g_{9/2}$ orbital, $\nu = 2$ and $\nu = 4$ multiplets are expected to appear from the break of one and two $J = 0$ pairs, respectively. In all three theoretical works the 6^+ , $\nu = 4$ level is calculated to lie below the 8^+ , $\nu = 2$ state, opening a fast decay path between states of different seniority that reduces the lifetime of the 8^+ level. Experimentally, the only seniority states unambiguously placed in the level scheme of ^{72}Ni are the yrast 2^+ , 4^+ , and 6^+ levels [12,13,25,26]. A few more γ rays have recently been

reported [25,26], of which a 199- and a 1069-keV transitions have been claimed to deexcite the so-sought-after 8^+ , $\nu = 2$ and 4^+ , $\nu = 4$ states. These assignments, though, are far from being conclusive owing to the limited statistics suffered by these works.

The present paper reports a wealthy set of new results on ^{72}Ni . This nucleus has been studied in a β -decay experiment performed at the RIKEN Nishina Center with the use of the BigRIPS and EURICA setups [27]. A total of 60 transitions have been attributed to the β decay of ^{72}Co to ^{72}Ni , and 21 new levels have been proposed with tentative assignment of spins and parities. As discussed later in the text, part of this information has been confirmed by exploring the β -decay chain from the progenitor ^{72}Fe and the β -delayed neutron-emission branch from ^{73}Co . As a result, an extended review of the low-lying structure of ^{72}Ni is presented and discussed.

This paper is organized as follows. In Sec. II the experimental setup is presented. Section III describes the data analysis and shows the comprehensive level scheme built analyzing the coincidence relations between the measured γ rays. In Sec. IV we provide experimental evidence for the existence of two β -decaying states in ^{72}Co . In Sec. V we discuss the results, showing the structures populated from the high-spin (part A) and low-spin (part B) isomers and the comparison with shell-model calculations (part C). A summary and conclusions are given in Sec. VI.

II. EXPERIMENTAL APPARATUS

The present experiment was carried out at the RI Beam Factory (RIBF) of the RIKEN Nishina Center, in Japan. A sequential acceleration system consisting of a linac injector (RILAC) and four ring cyclotrons (RRC-fRC-IRC-SRC) delivered a ^{238}U primary beam at 345 MeV/nucleon with a stable intensity of 10 pA. The nucleus ^{72}Co and other exotic species close to ^{78}Ni were produced in in-flight fission on a 3-mm Be target. The fission residues were first separated in the first stage of the BigRIPS spectrometer using two dipole magnets and a wedge-shaped achromatic degrader placed in between. This allowed for an improved identification through the standard ΔE - $B\rho$ -TOF method in the second stage of BigRIPS, as described in Ref. [28]. Event-by-event information on the atomic charge (Z) and mass-to-charge (A/Z) ratio of the nuclei was obtained from time-of-flight, position, and energy loss measurements exploiting fast plastic scintillators, parallel-plate avalanche chambers, and multi-sampling ionization chambers.

The exotic nuclei were then transported through the ZeroDegree spectrometer [29] to the EURICA β -decay spectroscopy station [27,30]. A variable-thickness Al degrader was placed in front of the setup to adjust the implantation depth of the nuclei in the Wide-range Active Silicon Strip Stopper Array for Beta and ion detection (WAS3ABi) [30]. In total, 8.84×10^5 implantation events were registered for ^{72}Co . WAS3ABi consisted of five double-sided silicon strip detectors (DSSSD) aligned along the beam axis. Each DSSSD detector comprised 2400 pixels of $1 \times 1 \times 1$ mm³ defined by 60 vertical and 40 horizontal strips. The array recorded position, time, and energy information on the implanted

residues and the electrons emitted in both β decay and internal conversion processes. Energy and time signals from each strip were read by standard analog electronics. Coincident γ rays were detected in the EURICA γ spectrometer [30], made of 12 seven-element high-purity germanium (HPGe) detectors from the decommissioned EUROBALL array [31]. The HPGe clusters were set up in packed isotropic geometry around the active stopper to increase the detection efficiency of the apparatus, which resulted in 11% at 662 keV after applying standard add-back procedures. Energy and time information of γ rays were recorded during an acquisition time window of 110 μs following the detection of an implantation or an electron. This allowed for the measurement of half-lives of isomeric nuclear states from several ns up to several hundred μs . Ancillary fast-timing detectors were also incorporated to extend the experimental sensitivity down to 100 ps: Two BC-418 plastic scintillators were placed upstream and downstream the active stopper, and 18 LaBr_3 scintillators of dimensions $\phi 1.5'' \times 2''$ were assembled in three groups of six individual detectors occupying the vacant slots of the EURICA spectrometer [32]. The fast plastics were additionally used to reject the secondary reaction products generated during the implantation of the nuclei. Events with a low-energy signal in the first plastic detector or a high-energy signal in the second one were excluded from the analysis.

III. RESULTS

The nuclei of ^{72}Co were correlated with all β particles registered in the triggering pixel and its adjacent cells during a maximum time of 5 s after the implantation event. The resulting activities were sorted as a function of time to extract the β -decay half-lives. Then β -delayed γ spectra were sorted by defining a nucleus- β correlation time window equal to five half-lives and a β - γ prompt-time coincidence of ~ 200 ns. The latter window could be adjusted up to 110 μs , depending on the half-lives of the daughter states. The remaining contribution from other nuclei, in particular the decay-chain successors, was evaluated in equivalent γ spectra sorted at longer times, typically set according to the known lifetimes of the daughter and grand-daughter nuclei. For further details on the experimental setup and the analysis procedure, the reader is referred to Refs. [33–36].

The singles β -delayed γ spectrum following the implantation of ^{72}Co is shown in the top part of Fig. 1. After subtracting contributions from other implanted residues and decay-chain daughters, the only background lines seen are either sum peaks arising from the strong 1194-454-843-1095-keV γ cascade or room background (asterisks). Transitions in ^{71}Ni (β_n) and ^{70}Ni (β_{2n}) are labeled with the final nucleus in parentheses. In total, 57 transitions have been attributed to the β decay of ^{72}Co to ^{72}Ni , of which only the 1095-, 843-, 454-, 1194-, 579-, 698-, and 1070-keV γ rays were reported in previous works [12,13,25,26]. An additional γ ray with energy of 199 keV was reported in Ref. [25]. It was interpreted as deexciting the (8^+) seniority-two state; however, we do not observe such a transition as shown in Fig. 1.

Most of the γ rays observed in the singles γ spectrum have been placed in the level scheme of ^{72}Ni with the

help of β -delayed γ - γ prompt coincidences, γ -ray intensity balances, and energy-sum matching conditions. Examples of γ - γ coincidence spectra for the decay of ^{72}Co to ^{72}Ni are shown in the bottom part of Fig. 1 and in Figs. 2 and 3. These have been built requiring a maximum time difference of 300 ns with the gated γ ray. Three additional transitions that do not clearly emerge from the background in Fig. 1 have been identified in the γ - γ coincidence analysis and are hence assigned to ^{72}Ni . Their energies are 689, 1108, and 1118 keV.

In some cases the comparison with the spectrum following the β -delayed neutron emission $^{73}\text{Co} \rightarrow ^{72}\text{Ni}$ has been helpful to define the placement of specific transitions. Examples of γ - γ coincidence spectra from this decay branch are shown in Fig. 4.

These rich spectroscopic data have allowed for a detailed extension of the excited levels in ^{72}Ni , reaching almost the neutron separation energy at 6891 keV [37]. Only 11 transitions have remained unplaced owing to ambiguous (or absent) γ -coincidence relations. These are listed in Table I together with their relative intensities (normalized to the intensity of the 1095-keV peak) and their coincidence relationships. It is worth anticipating that two well-defined structures at high and low spins have been identified in ^{72}Ni , each arising from a different β -decaying state in the mother nucleus. The corresponding partial level schemes are shown in Figs. 5 and 6. In the following, we explain how these groups of levels have been identified and separated.

The placement of new levels has been performed starting from well-established information. Among the known transitions, only the 1194-454-843-1095-keV cascade was correctly attributed to the (6^-)-(6_1^+)-(4_1^+)-(2_1^+)- 0^+ decay sequence. We confirm that the transitions at 1194, 454, 843, and 1095 keV form a single cascade depopulating the state at 3586 keV. As shown in the partial level scheme of Fig. 5, we find 6 additional transitions deexciting the 3586-keV state, with energies of 950, 579, 496, 411, 397, and 77 keV. These populate new levels at 2636, 3007, 3090, 3175, 3189, and 3509 keV, respectively. The 3509-keV level decays to the (4_1^+) state through a 1571-keV transition (see top panel of Fig. 3). Because no additional γ rays are observed feeding or depopulating the state, the placement has been defined only on the basis of the relative intensities of the 77- and 1571-keV transitions. The ordering of the other five cascades is fixed by coincidence information, γ -ray intensity balances, and energy-matching constraints. For instance, the transitions with energies of 579 and 371 keV, which are in mutual coincidence (see Fig. 2), add up to 950 keV and hence feed the 2636-keV level, which decays to the well-known (4_1^+) state via the 698-keV γ ray. The location of the intermediate level at 3007 keV is confirmed by the observation of other three deexciting transitions with energies of 1070, 615, and 684 keV. These populate the known (4_1^+) and (6_1^+) states and a new level at 2323 keV that decays only to the (2_1^+) state via a 1228-keV transition (see Fig. 2). The placement of the 2323-keV level is further fixed by the observation of the 579-684, 496-767, and 411-853 γ cascades decaying from the known (6^-) state. Similarly, the placement of the 3090-keV level is verified by the observation of an additional 1152-keV transition decaying to the (4_1^+) state (see second panel of Fig. 3).

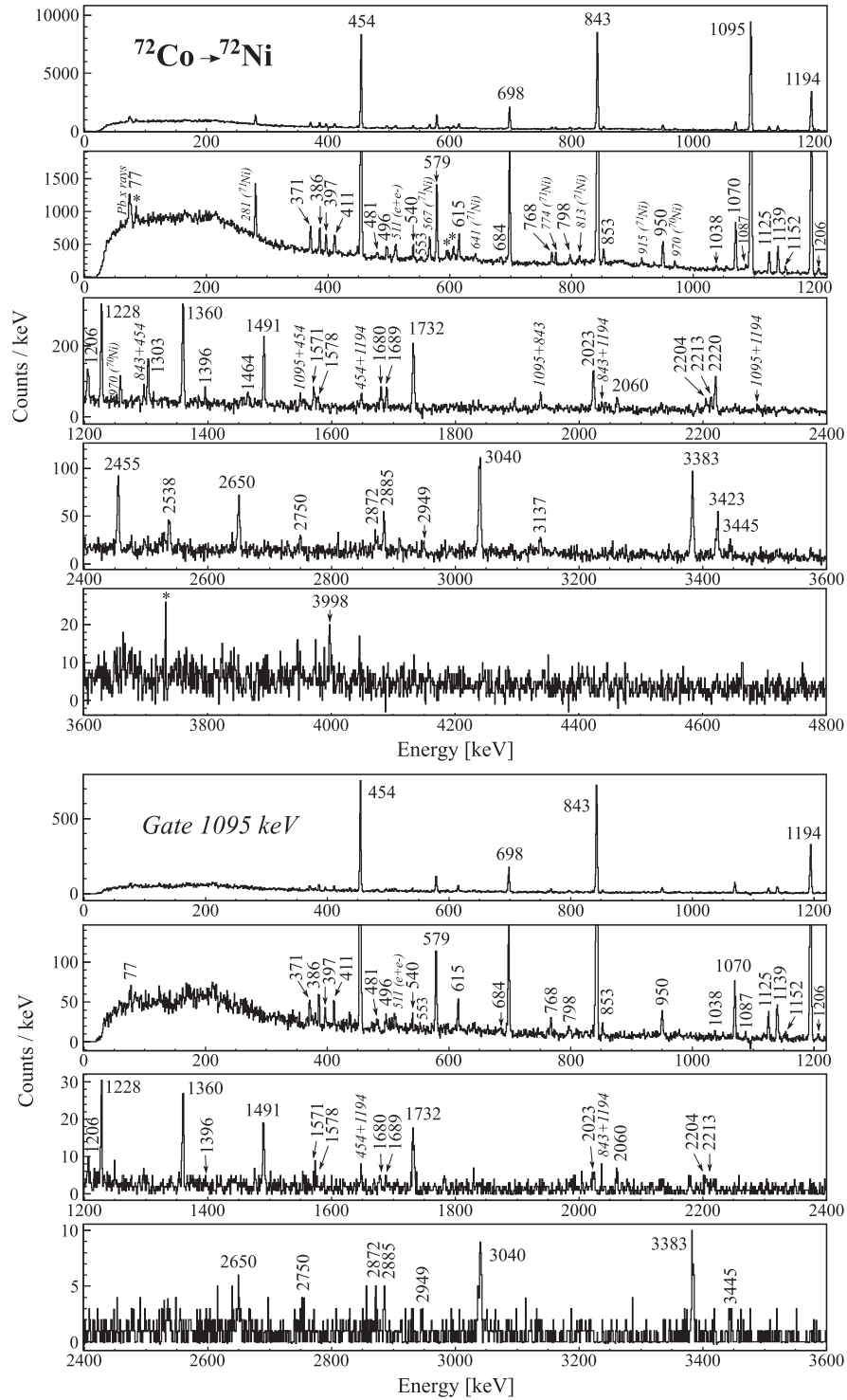


FIG. 1. (Top) β -delayed γ -ray energy spectrum following the implantation of ^{72}Co . The energy region from 0 to 1200 keV is presented for two ranges of the y axis to facilitate the observation of weak γ rays. Background contribution from other nuclei and decay-chain daughters is subtracted as indicated in the text. The γ -ray transitions attributed to ^{72}Ni are labeled with their energies, while those associated with ^{71}Ni and ^{70}Ni are indicated by the corresponding nucleus in parentheses. Background γ lines are shown as asterisks. Sum peaks arising from the strong 1194-454-843-1095-keV γ cascade are labeled with the two γ rays originating the peak. (Bottom) Same as before, but gated on the $(2_1^+) \rightarrow 0_1^+$ transition at 1095 keV.

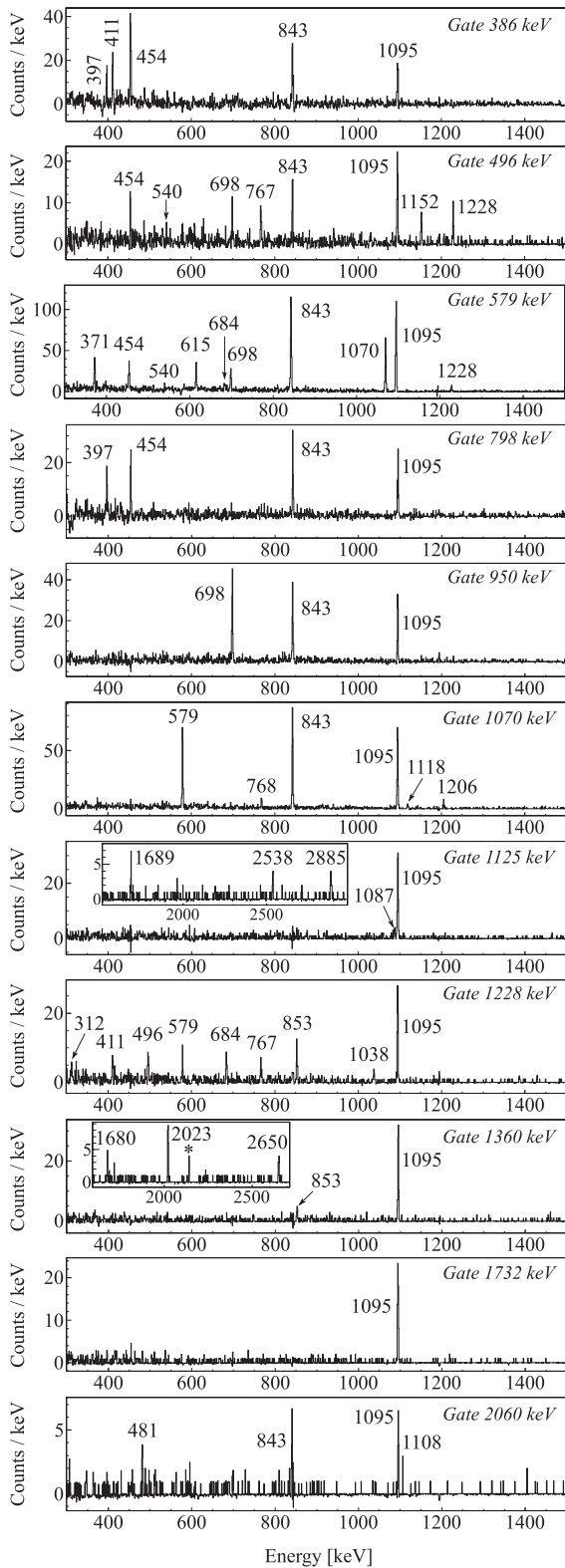


FIG. 2. Examples of β -delayed γ - γ coincidence spectra for the decay $^{72}\text{Co} \rightarrow ^{72}\text{Ni}$. From top to bottom, the spectra are gated on the 386-, 496-, 579-, 798-, 950-, 1070-, 1125-, 1228-, 1360-, 1732-, and 2060-keV γ rays. Transitions marked with an asterisk do not show mutual coincidence relations.

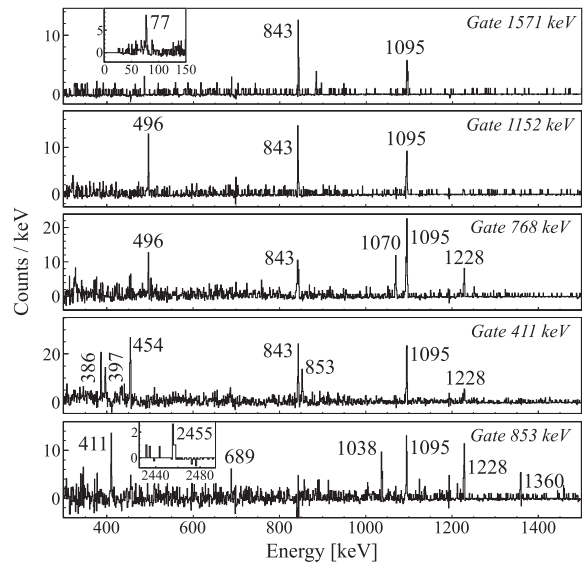


FIG. 3. β -delayed γ - γ coincidence spectra gated on the 1571-, 1152-, 768-, 411-, and 853-keV γ rays attributed to the decay $^{72}\text{Co} \rightarrow ^{72}\text{Ni}$. The spectra evince that the transitions at 411, 768, and 853 keV are double peaks associated with more than one γ cascade.

In the case of the 397-411-386 cascade, the γ -ray ordering has been fixed with the help of the β -delayed neutron-emission data from ^{73}Co . As shown in Fig. 4, the only transition of this cascade in mutual coincidence with the 1095-, 843-, and 454-keV γ rays in the β_n branch of ^{73}Co is the one at 386 keV. Because its only possible placement is on top of the $(6_1^+) - (4_1^+) - (2_1^+) - 0^+$ sequence, the newly observed 2778-keV level is most likely the sought-after (8^+) seniority-two state. Additional support comes from the almost negligible

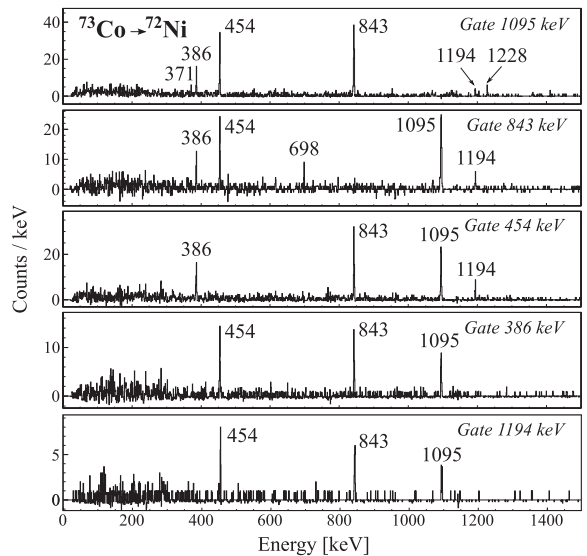


FIG. 4. β -delayed γ - γ coincidence spectra for the β_n decay $^{73}\text{Co} \rightarrow ^{72}\text{Ni}$. From top to bottom, the spectra are gated on the 1095-, 843-, 454-, 386-, and 1194-keV transitions.

TABLE I. List of γ -ray transitions associated to the β decay of ^{72}Co to ^{72}Ni that have not been placed in the level scheme of ^{72}Ni . The energies E_γ , relative intensities I_γ (normalized to the intensity of the 1095-keV peak), and coincidence relations are indicated.

E_γ (keV)	I_γ (%)	Coincident γ rays
553(3)	0.30(3)	698, 843, 1095
1303.5(16)	1.74(15)	—
1395.5(17)	0.29(4)	1095, 2204
1464(2)	0.58(6)	1360
2204.2(5)	0.29(4)	1095, 1396
2749.8(18)	0.31(5)	698, 843, 1095
2872(4)	0.56(7)	511, 852, 1095
2949(4)	0.34(5)	1095
3137(3)	0.50(7)	1095
3423(3)	1.44(15)	1054, 1681
3445(3)	0.50(7)	454, 1095

β feeding to this level following direct β decay from ^{72}Co [$I_\beta \leq 1.3(4)\%$, see Table III]. The order of the higher-lying 397- and 411-keV transitions has been fixed by the observation of a 798-keV γ line crossing the 411-386-keV cascade, in mutual coincidence with the 397-, 454-, 843-, and 1095-keV transitions (see Fig. 2). This unambiguously fixes the location of the 3189-keV level.

Only one transition with energy of 540 keV has been placed on top of the (6^-) state. The resulting level at 4126 keV also

deexcites via a 1118-keV transition to the 3007-keV state and via a 1490-keV decay to the 2636-keV level. Similarly, the placements of the levels at 3775 and 4213 keV are confirmed by the observation of deexciting transitions to the 3007- and 2636-keV levels, with energies of 768 and 1139 keV and 1206 and 1578 keV, respectively. The 4213-keV state is further connected to the 3175-keV level via a γ ray of 1038 keV. An additional γ ray with energy of 2750 keV is found in weak coincidence with the 698-, 843-, and 1095-keV transitions. Though it is more probably located above the 2636-keV level, the location of the resulting 5386-keV state is tentative and, for caution, we have preferred to include the 2750-keV γ ray in Table I rather than in the level scheme.

In the partial level scheme of Fig. 6, a set of γ rays found in coincidence with the well-established $(2^+) \rightarrow 0^+$ transition at 1095 keV are shown. These have energies of 1125, 1360, 1732, 2213, 3040, and 3383 keV and hence deexcite new levels at 2220, 2455, 2827, 3308, 4135, and 4478 keV. Of these, the 2220- and 2455-keV levels show direct ground-state decays. A new level at 3997 keV also decays directly to the ground state, deexcites to the (4_1^+) level through a 2060-keV transition, and feeds the 3308-keV level via a 689-keV γ ray (see bottom panel of Fig. 3). The 3308-keV level feeds, in addition to the 1095-keV state through the 2213-keV γ ray, the 2220- and 2455-keV levels via the 1087- and 853-keV transitions, respectively. The 4135-keV state also deexcites to the 2455-keV level via a 1680-keV γ ray, and the 4478-keV level decays to the 2455- and 3997-keV states via the 2023- and 481-keV transitions, respectively. Three more transitions

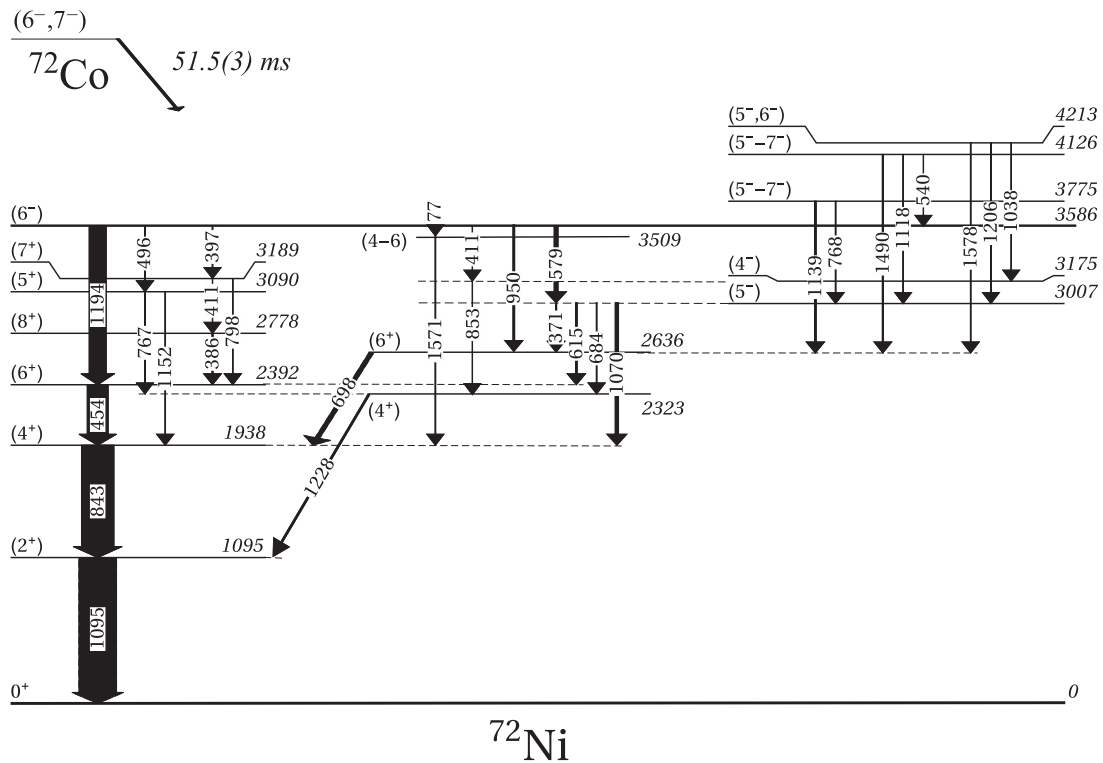


FIG. 5. Partial level scheme of ^{72}Ni attributed to the β decay of the high-spin isomer of ^{72}Co . Tentative spin and parities J^π of the observed states are indicated on the left part of the levels. Widths of the arrows are proportional to their absolute intensities (i.e., normalized to the number of implantations of ^{72}Co). See text for details.

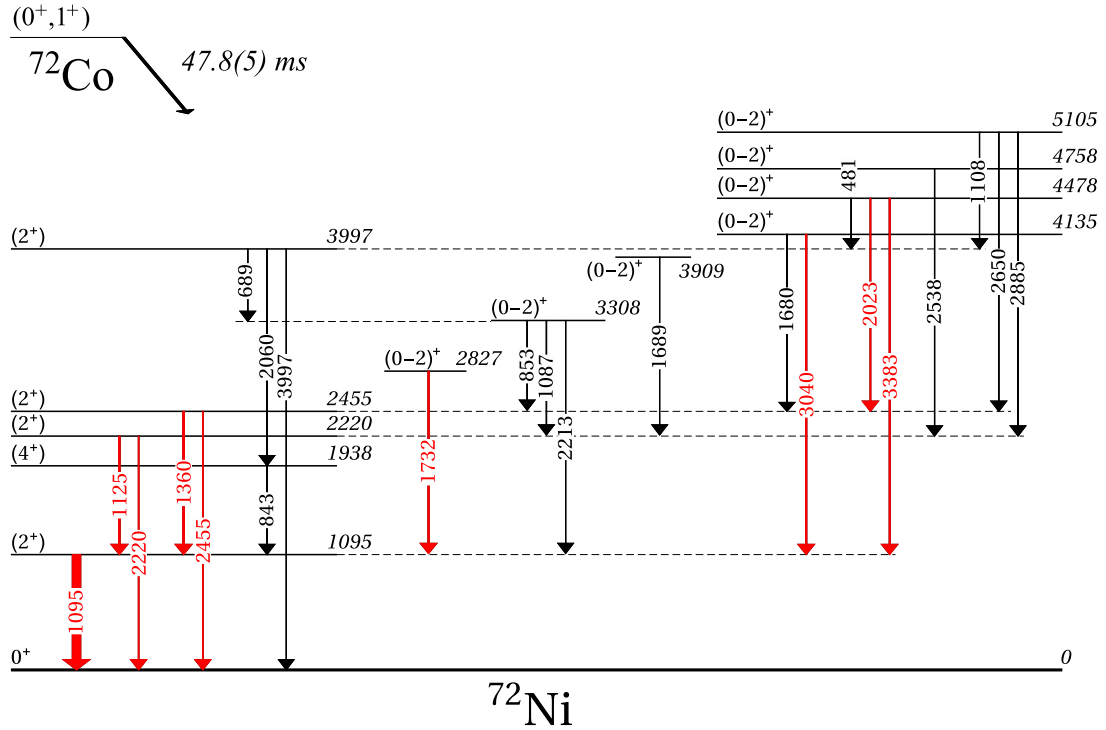


FIG. 6. Partial level scheme of ^{72}Ni attributed to the β decay of the low-spin isomer of ^{72}Co . Tentative spin and parities J^π of the observed states are indicated on the left part of the levels. Widths of the arrows are proportional to their absolute intensities (i.e., normalized to the number of implantations of ^{72}Co). Transitions labeled in red stand for γ rays observed following implantations of both ^{72}Co and ^{72}Fe . See text for details.

are placed on top of the level at 2220 keV. These have energies of 1689, 2538, and 2885 keV and thus deexcite from new levels at 3909, 4758, and 5105 keV. In the case of the 5105-keV state, two additional transitions with energies of 2650 and 1108 keV feed the 2455- and 3997-keV levels. All these coincidence relations can be seen in Fig. 2, where the γ spectra gated on the 1125-, 1360-, and 2060-keV γ rays (deexciting levels which show direct ground-state decay) are shown.

It is worth noting that the 411-, 768-, and 853-keV transitions have been located twice in the level scheme. These assignments are based on their coincidence relationships, which clearly evince more than one coincident cascade (see Fig. 3). For instance, the 768(767)-keV double peak is part of the 496-767-1228-1095- and 768-1070-843-1095-keV sequences decaying from the 3586- and 3775-keV levels, respectively. The 411- and 853-keV γ lines are part of a cascade feeding the (4_2^+) state at 2323 keV, while at the same time are in the decay paths of the 3586- and 3997-keV states, respectively.

IV. CONFIRMING THE EXISTENCE OF TWO β -DECAYING STATES IN ^{72}Co

In the early work of Mueller *et al.* [38], two β -decaying states were observed in both ^{68}Co and ^{70}Co . While the short-living isomer was interpreted as the $(\pi f_{7/2}^{-1} \nu g_{9/2}^{+1,+3})$ ground state, the long-living state was tentatively attributed

to the coupling of the single-particle configurations $\pi f_{7/2}^{-1}$ and $(\nu p_{1/2}^{-1} \nu g_{9/2}^{+2,+4})$. This assignment was based on systematics with the neighboring ^{66}Co isotope, where a tentative (3^+) ground state was proposed from the nonobservation of ground-state β feeding to ^{66}Ni [38,39]. The β -decaying $(1/2^-)$ levels found in ^{69}Ni [16,40] and ^{71}Ni [41–43] reinforce this assumption. However, the discovery of a low-energy β -decaying intruder state in ^{67}Co [44], interpreted as a proton-core excitation to the $\Omega^\pi = 1/2^-$ deformed shell of the $p_{3/2}$ orbital, opened up the possibility for other proton-neutron couplings involving deformed shapes. Based on this argument and on the strong ground-state feeding observed in the β decay of ^{66}Fe to ^{66}Co , Liddick *et al.* [45] pointed to a plausible $J^\pi = (1^+)$ assignment arising from the coupling of a deformed $(1/2^-)$ neutron to the observed $(1/2^-)$ proton state in ^{67}Co . Yet the recent observation of negative-parity states in the β decay of the ^{68}Co low-spin isomer has opened the door for additional couplings. For instance, the descending $\Omega^\nu = 1/2^+$ and $3/2^+$ shells of the $g_{9/2}$ orbital can join to the deformed $(1/2^-)$ proton state to produce a $J^\pi = (1^-)$ or (2^-) isomer, as suggested by Flavigny *et al.* [8].

In ^{72}Ni , the observation of several levels with direct decay to the ground state suggests that a low-spin structure is populated simultaneously in the β decay of ^{72}Co . This provides experimental support for the presence of the low- J β -decaying isomer also at mass $A = 72$. We have confirmed its existence through the study of the β -decay sequence

TABLE II. List of levels of ^{72}Ni observed in the β decay of the high-spin isomer of ^{72}Co . The energy E_{level} , the tentative spin and parity J^π , the apparent β feeding I_β , and the calculated $\log ft$ value are summarized for each level. As well, the energies E_γ of the deexciting γ -ray transitions and their absolute intensities I_γ are indicated. Note that the I_β and $\log ft$ values correspond to upper and lower limits, respectively.

E_{level} (keV)	^{72}Ni high-spin isomer, $t_{1/2} = 51.5(3)$ ms				
	J^π	I_β (%)	$\log ft$	E_γ (keV)	I_γ (%)
1094.8(11)	(2 ⁺)	—	—	1094.8(11)	101(9)
1937.6(12)	(4 ⁺)	2(6)	—	842.7(11)	95(9)
2322.8(18)	(4 ⁺)	—	—	1227.9(13)	4.2(4)
2391.7(13)	(6 ⁺)	2(4)	—	454.3(9)	62(6)
2635.8(17)	(6 ⁺)	1.5(11)	6.3(4)	698.2(11)	18.8(18)
2778(2)	(8 ⁺)	1.3(4)	6.37(17)	386.2(18)	3.3(3)
3007.1(12)	(5 ⁻)	3.8(10)	5.87(16)	371.4(19)	3.0(3)
				615.1(18)	4.8(5)
				684(4)	1.24(13)
				1069.7(13)	9.8(9)
3090(2)	(5 ⁺)	0.03(23)	—	767(2)	1.21(18)
				1152.1(18)	1.05(12)
3175(3)	(4 ⁻)	0.05(31)	—	852.9(19)	1.8(3)
3189(2)	(7 ⁺)	1.7(4)	6.19(15)	411(2)	2.0(4)
				798(4)	2.0(2)
3509(3)	(4-6)	1.14(13)	6.3(12)	1571(2)	1.14(13)
3586.0(12)	(6 ⁻)	70(6)	4.50(12)	76.7(8)	—
				397(2)	2.4(2)
				411(2)	0.90(12)
				496(2)	2.2(2)
				578.9(12)	11.4(11)
				950.2(17)	5.3(5)
				1194.2(12)	50(5)
3775.1(18)	(5 ⁻ 7 ⁻)	6.9(7)	5.47(13)	768(2)	1.5(3)
				1139.3(13)	5.4(5)
4126.1(17)	(5 ⁻ 7 ⁻)	5.8(5)	5.48(13)	540.0(16)	2.3(2)
				1118.1(13)	0.56(7)
				1490.5(12)	3.0(3)
4213.0(16)	(5 ⁻ ,6 ⁻)	3.1(3)	5.74(13)	1038(2)	0.83(10)
				1206(2)	1.53(17)
				1578(2)	0.70(9)

$^{72}\text{Fe} \rightarrow ^{72}\text{Co} \rightarrow ^{72}\text{Ni}$. As for ^{68}Co [8] and ^{70}Co [11], the low-spin isomer in ^{72}Co can be isolated in a natural way following the β decay of the ground state of its Fe precursor. In the present experiment, a total of 5×10^3 implantation events were registered in the WAS3ABi active stopper for ^{72}Fe . Though the limited statistics prevent us from performing a statistically significant half-life measurement, a qualitative analysis of the γ -ray transitions associated with ^{72}Ni is possible. Figure 7 shows the singles β -delayed γ spectrum of ^{72}Fe including ion- β correlations up to 350 ms. The well-known (2₁⁺) \rightarrow 0⁺ γ ray at 1095 keV is clearly visible. Moreover, the transitions at 1125, 1302, 1360, 1732, 2023, 2219, 2454, 3040, and 3384 keV emerge modestly from the background. Though no coincidence relations can be extracted from the present data, the appearance of these γ lines in the β -delayed γ spectrum of ^{72}Fe confirms their connection to

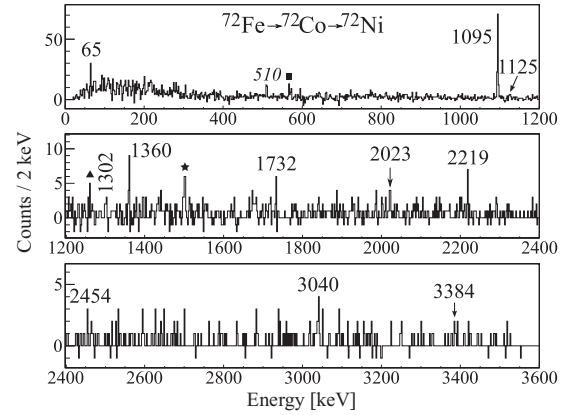


FIG. 7. β -delayed γ spectrum of ^{72}Fe extended up to 350 ms after the ion implantation. The γ rays marked in normal font are attributed to ^{72}Ni , while transitions assigned to the β_n (^{71}Ni) and β_{2n} (^{70}Ni) grand-daughters are indicated as solid squares and solid triangles, respectively. The star indicates a transition associated with the decay of ^{72}Fe to ^{72}Co .

the low-spin isomer. Besides this, one new transition with energy of 65 keV has been identified for the first time. Because it only appears in the β -delayed γ spectrum of ^{72}Fe when extending the correlation time window to include the decay of the daughter ^{72}Co , we tentatively assign it to the deexcitation of a low-spin state in ^{72}Ni .

Tables II and III list the levels proposed as arising from the decay of the high- and low-spin isomers, respectively. These have been separated according to the information obtained in the β decay of ^{72}Fe and the discussion on J^π assignments reported in Sec. V. The tentative spins and parities, apparent β feedings, and $\log ft$ values are also indicated. Note that the apparent β feedings correspond to upper limits as possible γ feeding from higher-lying states [46] has not been considered; hence, the $\log ft$ values are lower limits. To extract these values, we have assumed that the feeding to the states populated by both isomers, i.e., the ground state and first (2⁺) level, originates only from the low-spin isomer. The Q_β value has been taken from Ref. [47]. The γ transitions deexciting each level and their absolute intensities I_γ (normalized to the number of β decays of the initial state) are shown in the last two columns of the tables.

In the lighter Co isotopes, the half-lives of the low-spin states were determined through γ -ray time-decay analysis, with resulting values of $t_{1/2} = 1.6(3)$ s for ^{68}Co and $t_{1/2} = 500(180)$ ms for ^{70}Co [38]. In Fig. 8 we show fits to γ -gated activity curves for the decay $^{72}\text{Co} \rightarrow ^{72}\text{Ni}$. The left panel displays the decay spectrum for the transitions at 1680, 1689, 1732, 2023, 2538, 2650, 2885, 3040, and 3383 keV, which are attributed to the decay of the low-spin isomer in Table III, while the right one shows the time behavior of the (6₁⁺) \rightarrow (4₁⁺) transition at 454 keV, which exclusively follows the decay of the high-spin state. At variance with ^{68}Co and ^{70}Co , the measured half-lives in ^{72}Co are very similar, $t_{1/2}^{\text{low}} = 47.8(5)$ ms and $t_{1/2}^{\text{high}} = 51.5(3)$ ms. Note that the half-life of the high-spin isomer is in agreement with the recently proposed value of 52.8(16) ms [48].

TABLE III. List of levels of ^{72}Ni observed in the β decay of the low-spin isomer of ^{72}Co . The energy E_{level} , the tentative spin and parity J^π , the apparent β feeding I_β , and the calculated $\log ft$ value are summarized for each level. As well, the energies E_γ of the deexciting γ -ray transitions and their absolute intensities I_γ are indicated. Note that the I_β and $\log ft$ values correspond to upper and lower limits, respectively.

E_{level} (keV)	^{72}Ni low-spin isomer, $t_{1/2} = 47.8(5)$ ms				
	J^π	I_β (%)	$\log ft$	E_γ (keV)	I_γ (%)
0	(0 ⁺)	$\leq 42(13)$	5.25(16)	—	—
1094.8(11)	(2 ⁺)	13(13)	5.6(5)	1094.8(11)	48(20)
1937.6(12)	(4 ⁺)	2(6)	—	842.7(11)	1.3(3)
2220.0(13)	(2 ⁺)	4.4(10)	5.90(14)	1125.0(13)	7.5(13)
				2220.0(18)	3.7(7)
2454.9(13)	(2 ⁺)	0.3(7)	—	1359.8(15)	7.9(14)
				2455.2(19)	3.5(6)
2827(2)	(0 - 2) ⁺	6.5(12)	5.63(14)	1732.1(18)	6.5(12)
3307.7(12)	(0 - 2) ⁺	5.3(9)	5.64(14)	852.9(19)	1.9(4)
				1086.8(19)	2.2(4)
				2212.9(17)	1.2(2)
3909(2)	(0 - 2) ⁺	1.4(3)	6.11(15)	1688.9(16)	1.4(3)
3997.2(10)	(2 ⁺)	0.1(3)	—	689(2)	—
				2060(3)	1.3(3)
				3997.5(13)	0.9(2)
4134.8(17)	(0 - 2) ⁺	8.2(15)	5.30(15)	1680(2)	1.9(4)
				3039.6(19)	6.3(11)
4477.9(16)	(0 - 2) ⁺	12(2)	5.07(15)	481(4)	2.1(4)
				2023.0(17)	4.4(8)
				3383.4(18)	5.4(10)
4758(2)	(0 - 2) ⁺	1.6(3)	5.89(15)	2538(3)	1.6(3)
5105.0(19)	(0 - 2) ⁺	4.6(8)	5.36(15)	1108(2)	—
				2650(3)	2.9(5)
				2885.0(15)	1.7(3)

Finally, it is worth noting the presence of the 1302-keV γ line in the β -delayed γ spectrum following the implantation of ^{72}Fe ; see Fig. 7. This is most likely the 1303-keV transition observed in the β decay of ^{72}Co ; see Fig. 1 and Table I. Because this γ ray shows no mutual coincidence with any other transition assigned to ^{72}Ni , it may feed either an isomer

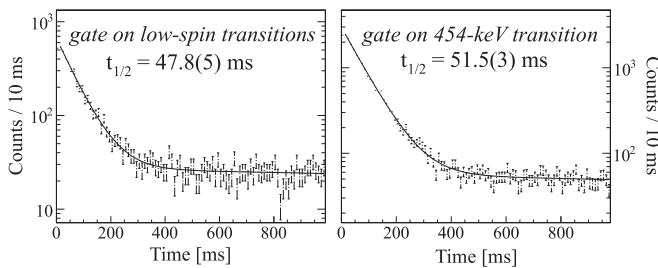


FIG. 8. (Left) β -decay activity curve gated on some γ -ray transitions attributed to the decay of the low-spin isomer in ^{72}Co . The transitions included have energies of 1680, 1689, 1732, 2023, 2538, 2650, 2885, 3040, and 3383 keV. (Right) Same as the previous one, but for the $(6_1^+) \rightarrow (4_1^+)$ γ ray at 454 keV, assigned to the decay of the high-spin isomer of ^{72}Co .

or an excited 0⁺ state that decays by internal conversion or electron-positron pair production to a lower-lying 0⁺ level. The strong branching ratio to the ground state, $I_\beta \leq 42(13)\%$, is consistent with the latter interpretation.

V. DISCUSSION

The discussion on the proposed spins and parities is organized in two sections dedicated to the high-spin (A) and low-spin (B) groups, respectively. In Sec. C the newly reported levels are compared with shell-model calculations in the neutron $f_{5/2}p_{3/2}p_{1/2}g_{9/2}$ model space, employing the single-particle energies and phenomenological effective interaction reported in Ref. [23]. Because ^{72}Ni has a 28-magic proton core, this reduced model space is expected to be sufficient to successfully reproduce the energy of the nearly spherical states.

A. β decay of the high-spin isomer

The strong β feeding to the 3586-keV level, $I_\beta \leq 70(6)\%$, clearly indicates the occurrence of an allowed Gamow-Teller transition from the lowest $\pi f_{7/2}^{-1} \nu g_{9/2}^{+5}$ state in ^{72}Co , which is expected to have $J^\pi = (6^-)$ or (7^-) by analogy with lighter Ni isotopes [38]. Because the most favored decay requires the transformation $\nu f_{5/2} \rightarrow \pi f_{7/2}$, the wave function of this level is most probably built on the particle-hole excitation $\nu f_{5/2}^{-1} \nu g_{9/2}^{+5}$, and thus the spin and parity of the state is either (6^-) or (7^-) .

As shown in Fig. 5, the nonobservation of a transition connecting the 3586-keV state with the newly reported (8^+) level suggests that the spin and parity of the first is more likely $J^\pi = (6^-)$. This is in agreement with the recent (6^-) assignment for the analogous 3592-keV state in ^{70}Ni [9]. The level at 3189 keV is fed from the (6^-) state and deexcites to the (8^+) and (6_1^+) levels. This points to a (7^+) assignment, which is supported by the low β feeding to the state, $I_\beta \leq 1.7(4)\%$ (see Table II). As well, a weak γ line with energy of 553 keV is found in coincidence with the 698-, 843-, and 1095-keV transitions. Based on energy summing, this transition can very likely connect the (7^+) state with the 2636-keV level; however, we have not placed it in the level scheme owing to missing coincidence relations with the 397-keV transition (see Table I). Apart from this and other weak decays, the 2636-keV state is directly fed from the (6^-) level via the 950-keV transition (see Fig. 5), while it only deexcites to the (4_1^+) state. This points to a plausible (6_2^+) assignment that is also supported by its large $\log ft \geq 6.3(4)$.

The intense 579-keV γ line connects the (6^-) level with the state at 3007 keV. As shown in the corresponding γ -gated spectrum of Fig. 2, the main transitions deexciting this level, at 615 and 1070 keV, decay to the previously known (6_1^+) and (4_1^+) states, while the weaker transitions at 371 and 684 keV decay to the (6_2^+) and 2323-keV levels, respectively. The 2323-keV level decays solely to the (2_1^+) state through the prompt 1228-keV transition, while it is not directly fed from the (6^-) level, thus pointing to a (4_2^+) assignment. A weak 312-keV transition observed in the γ spectrum gated on the 1228-keV peak (see Fig. 2) might indicate a certain degree of mixing between the

(6_2^+) and (4_2^+) states. This γ line is not included in the level scheme of Fig. 5 nor in Table I because it is not observed in the singles β -decay γ spectrum of Fig. 1. Moreover, its mutual coincidence with the 950- and 1095-keV γ rays, belonging to the same γ cascade to the ground state, has not been verified (see Figs. 1 and 2). An upper limit for its intensity can be extracted from the coincidence spectrum gated on the 950-keV γ ray, resulting in less than 7% of the 698-keV γ -ray intensity.

Note that the (4_2^+) state was erroneously located at 2164 keV in Ref. [26] owing to incomplete coincidence information on the 1070-keV transition, which is now placed deexciting the 3007-keV state (see Fig. 2 for coincidence relations). Such a decay pattern limits the spin of the 3007-keV state to $J = 4-6$. Because the 4^+ and 6^+ candidates related to seniority have already been identified, we assume this state is either a member of the ($\nu p_{1/2}^{-1} \nu g_{9/2}^5$) multiplet, hence with $J^\pi = (4^-)$ or (5^-), or the first (5^+) level, which is predicted to lie at 3015 keV by the shell-model calculations of Ref. [23] (see the following discussion in Sec. VC). None of them should be fed in the β decay of the high-spin isomer given the forbiddenness of the respective β transitions. This is in agreement with the measured β branching ratio for the 3007-keV level, $I_\beta \leq 3.8(10)\%$. Considering that the 615- and 371-keV transitions to the (6^+) states are observed, we dismiss the $J^\pi = (4^-)$ assignment. The 3007-keV level is also populated from higher-lying levels at 4213, 4126, and 3775 keV. Because their corresponding $\log ft$ values are 5.74(13), 5.48(13), and 5.47(13), they are most probably higher-lying members of the allowed ($\nu f_{5/2}^{-1} \nu g_{9/2}^{+5}$) multiplet. In ^{70}Ni , transitions connecting the ($\nu f_{5/2}^{-1} \nu g_{9/2}^{+5}$) (6^-) and (7^-) candidates with the ($\nu p_{1/2}^{-1} \nu g_{9/2}^5$) (5^-) level have recently been observed [9,11], pointing to a sizable mixing of both configurations. Based on this, we propose a tentative $J^\pi = (5^-)$ for the 3007-keV state. Additional support comes from the resemblance with the analogous candidates in lighter Ni isotopes ($E(5^-) = 2848$ keV in ^{68}Ni [38] and $E(5^-) = 2912$ keV in ^{70}Ni [9,11]).

The level at 3090 keV is fed from the (6^-) state through the 496-keV transition and deexcites to the (4_1^+) and (4_2^+) levels via the 1152- and 767-keV γ rays. Its negligible β feeding supports a $J^\pi = (5^+)$ or (4^-) assignment. Establishing the decay of this state to the (6_1^+) and (6_2^+) levels is difficult because the connecting transitions would have the same energies as the very intense 698- and 454-keV γ rays; however, because these peaks can be clearly seen in coincidence with the 496-keV transition (see Fig. 2), a $J^\pi = (5^+)$ assignment is preferred. It is worth noting that the 454- and 698-keV transitions do not show a clear coincidence relationship between them, and consequently, the decay branches from the 3090-keV level to the (6_1^+) and (6_2^+) states have not been indicated in the level scheme of Fig. 5. Moreover, from the present γ - γ coincidence information it is not possible to establish whether the 3090-keV level decays only to one of the two (6^+) states or to both of them. The level at 3175 keV also has a null β feeding (see Table II) and it only decays to the (4_2^+) level, so we propose this as the $J^\pi = (4^-)$ member of the ($\nu p_{1/2}^{-1} \nu g_{9/2}^5$) multiplet. This tentative location compares well with the excitation energy of the corresponding (4^-) state in ^{68}Ni at 3119 keV [49]. The only

remaining level below the (6^-) state is the one at 3509 keV. Its spin is constrained to $J = (4-6)$ based on the observation of a unique prompt γ decay to the (4_1^+) state.

As suggested before, the states at 3586, 3775, 4126, and 4213 keV belong more likely to the allowed ($\nu f_{5/2}^{-1} \nu g_{9/2}^{+5}$) multiplet. Because the β -decay spin-parity rules constrain the decay of the ($6^-, 7^-$) high-spin β -decaying isomer of ^{72}Co to the (5^-), (6^-), and (7^-) members, the appearance of sizable β feeding to four levels may be indicative of strong mixing between the ($\nu f_{5/2}^{-1} \nu g_{9/2}^{+5}$), ($\nu p_{1/2}^{-1} \nu g_{9/2}^{+5}$), and ($\nu p_{3/2}^{-1} \nu g_{9/2}^{+5}$) configurations. Highly mixed negative-parity states have already been observed in the valence mirror symmetry nuclei (see, for instance, Ref. [50]). While the 3775- and 4126-keV states can have $J^\pi = (5-7^-)$, the spin and parity of the 4213-keV level is constrained to (5^-) or (6^-) based on the observation of the 1038-keV transition to the (4^-) candidate.

B. β decay of the low-spin isomer

We start from the states with energies of 1095, 2220, 2455, and 3997 keV. The direct decays to the ground state suggest that their spins are more likely $J = (1)$ or (2), though a (3^-) assignment cannot be definitely ruled out because direct ground-state decays from 3^- levels have previously been reported in the region, particularly in ^{64}Ni [51]. As well, the (3^-) candidate in ^{68}Ni has recently been observed following β decay of the low-spin isomer of ^{68}Co [8]. We have to stress, though, that typical branching ratios of direct ground-state γ transitions in ^{72}Ni are well above the 30%, while the $3^- \rightarrow 0^+$ transition in ^{64}Ni only amounts to 11% [51]. Furthermore, no direct decay connecting the (3^-) level to the ground state has been observed in ^{66}Ni and ^{68}Ni [49]. Based on this, we tentatively dismiss the $J = 3$ spin assignment. A tentative $J^\pi = (2^+)$ is preferred because the first $J^\pi = (1^+)$ level can only be built through core excitations across $Z = 28$ or $N = 50$, leading to a higher excitation energy. In addition, the energies of the calculated $J^\pi = (1^-)$ and (2^-) states (at 3550 and 3401 keV, respectively) are about 1 MeV above the 2455-keV experimental level and 500 keV below the 3997-keV one.

In Table III, apparent β feedings and $\log ft$ values for the states attributed to the decay of the low-spin isomer are shown. Note the rather hindered decays to the (2^+) candidates, which are at variance with the strong branching ratios measured to the lowest-lying (2^+) states in ^{68}Ni and ^{70}Ni [8,11,38], and the significant population of the ground state, $I_\beta \leq 42(13)\%$, which is 3 times greater than in the β decay of the low-spin isomer of ^{70}Co [11]. Because we do not expect important contributions from missing feeding, our observations suggest a $J^\pi = (0^+)$ or (1^+) character for the low-spin isomer. Such spin and parity arises most probably from the coupling of the deformed proton and neutron configurations already suggested by Liddick *et al.* in ^{68}Co [45].

The spin and parities of the daughter levels at 2827, 3308, 3909, 4135, 4478, 4758, and 5105 keV, decaying solely to the (2^+) candidates, are constrained to $J^\pi = (0^+)$, (1^+), or (2^+) for allowed β transitions. It should be noted, however, that other spins and parities cannot be completely discarded: The initial state might arise from different deformed pn couplings or from

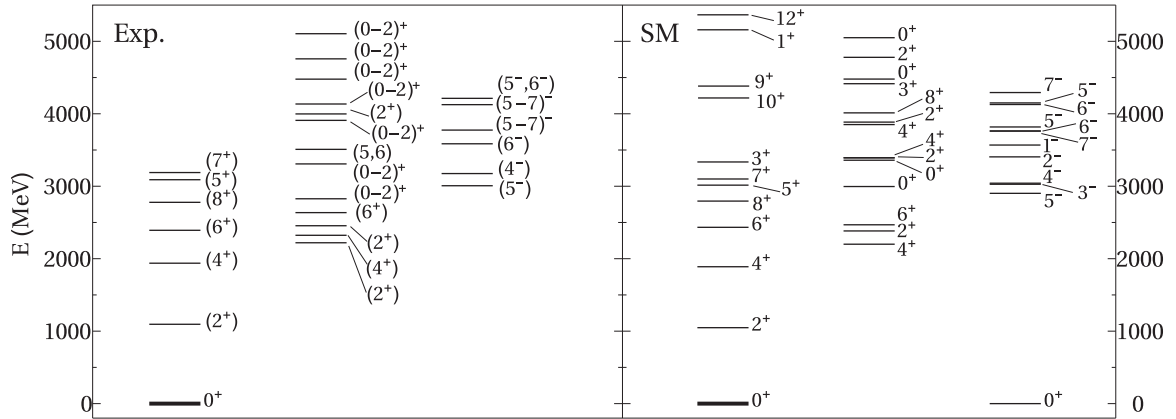


FIG. 9. (Left) Experimental level scheme of ^{72}Ni deduced from the present work. (Right) Level scheme of ^{72}Ni as predicted by the shell-model calculations described in Ref. [23]. In both cases, the levels are separated in three groups: yrast states, yrare levels, and negative-parity states.

a single neutron particle-hole excitation, and the final levels which show low β feedings can have spin and parity (1^-), (2^-), or (3^-) arising from first-forbidden β transitions. In the following, we discuss the different scenarios from comparison with shell-model calculations.

C. Comparison with shell-model calculations

In Fig. 9 we show experimental (left panel) and calculated (right panel) levels in ^{72}Ni . The calculated levels have been obtained with the shell-model code ANTOINE [52], using the effective single-particle energies and phenomenological interaction of Ref. [23] in the neutron fpg model space. For the yrast states the accuracy of the calculations is less than 100 keV, indicating that their structure can be well understood in terms of elementary neutron excitations. In the case of the (2_2^+) level, the experimental energy is 163 keV smaller than the theoretical one, suggesting that its wave function is also well described with the present neutron model space. Because the shell-model calculations predict a 75% contribution of the normal configuration $g_{9/2}^{+4}$ to the total wave function, this is more likely the 2^+ level arising from the breaking of two $g_{9/2}$ neutron pairs or from a combination of one and two broken $\nu g_{9/2}$ pairs. The second (4^+) level at 2323 keV lies at a slightly higher energy than the one predicted by the shell model, at 2200 keV. As a result there is an inversion of the experimental (2_2^+) and (4_2^+) states with respect to the theoretical predictions. This still supports their spherical-like structure because the accuracy of our shell-model calculations is below 200 keV. A similar situation applies for the (6_2^+) level, with the experimental energy 168 keV above the calculated value. Accordingly, the separation between the first two (6^+) levels is larger than expected, with the (2_3^+) candidate lying below the (6_2^+) level.

Note that the experimental energy of the tentative (2_3^+) state, 2455 keV, is almost 1 MeV below the shell-model calculation at 3392 keV. Theoretically, this level is composed by the two-neutron excitation from $p_{1/2}$ to $g_{9/2}$ (30%), by the $p_{1/2}^{-1}p_{3/2}^{-1}g_{9/2}^{+6}$ (14%) and $p_{1/2}^{-1}f_{5/2}^{-1}g_{9/2}^{+6}$ (12%) excitations,

and by the normal $g_{9/2}^{+4}$ configuration (11%). However, the large overestimation of the shell-model predictions suggests a significantly modified wave function or a different J^π assignment. In the previous section we commented that a possible $J^\pi = (3^-)$ nature cannot be completely ruled out on the only basis of the observation of the direct ground-state transition. Though the null β feeding to this level is consistent with a $J^\pi = (3^-)$ assignment, the discrepancy with the shell-model calculations of Ref. [23], which predict the 3^- level almost 600 keV above, leaves no clear interpretation for this state. In ^{68}Ni and ^{70}Ni , intruder levels attributed to strongly deformed bands have recently been observed [7,9], and their energies have been positively predicted by the Monte Carlo shell-model calculations of Tsunoda *et al.* [2] after explicitly including proton excitations across the $Z = 28$ shell gap. These crossed-core excitations have also been pointed to as the main factor in the development of deformation in $40 \leq N \leq 50$ nuclei below Ni (see Ref. [53] and references therein) and are further expected to stabilize low-lying deformed shapes in ^{72}Ni [2]. The dramatic overestimation of the (2_3^+) level energy when using the neutron fpg model space, thus, might be ascribed to the omission of such proton excitations. However, the fourth (2^+) level at 3997 keV is in good agreement with its theoretical counterpart at 3885 keV, though, based on the same arguments, a $J^\pi = (3^-)$ assignment is not definitely ruled out.

For the (5_1^-) and (4_1^-) levels, the calculated energies at 2902 and 3042 keV compare well with the experimental values at 3007 and 3175 keV, respectively. They can be reliably attributed to the excitation of a $p_{1/2}$ neutron to the $g_{9/2}$ shell based on the composition of their wave functions, with 66% and 69% percentage of this configuration each. The shell-model calculations overestimate the energy gap to the next group of negative-parity states, which have been attributed to the $\nu f_{5/2}^{-1}\nu g_{9/2}^5$ multiplet in Sec. V A. These present a sizable contribution from the neutron $p_{1/2}^{-1}g_{9/2}^5$ excitation, being typically above 10%. Note that the predicted mixing of configurations supports the observation of the strong 579-keV transition connecting the $\nu f_{5/2}^{-1}g_{9/2}$, (6^-) state with the $\nu p_{1/2}^{-1}g_{9/2}$, (5^-) level.

Regarding the low- J states, the energy of the first $(0-2)^+$ level, 2827 keV, matches well with the energy calculated for the second 0^+ state, at 2996 keV. However, the 0_2^+ level has a similar composition to that of the 2_3^+ state, which has not been successfully interpreted in terms of neutron excitations. If belonging to the same band, by analogy one would expect its experimental counterpart to be approximately 1 MeV below the calculated level, i.e., at about 2000 keV. However, in such a case its decay to the 2_1^+ state would have been observed. If the (0_2^+) level is positioned close enough to the (2_1^+) state, its decay will preferentially (or uniquely) proceed to the ground state via an $E0$ transition, which is not detectable with the present setup.

For the second $(0-2)^+$ level there are three theoretical states whose energies match the experimental value of 3308 keV: The 3_1^+ at 3335 keV, the 0_3^+ at 3359 keV, and the 4_3^+ at 3392 keV. The β feeding to the 3308-keV level results in a $\log ft > 5.64(14)$ and suggests that it might be fed via an allowed Gamow-Teller transition from the low-spin isomer; however, because the intensity of the feeding γ ray at 689 keV has not been extracted from the present data set (see Table III), this value is a lower limit. This, together with the close proximity between the theoretical $J = 0^+$, 3^+ , and 4^+ levels, hinders a firm assignment of spin for the initial state. Note that the 3308-keV level is also a good $J^\pi = (3^-)$ candidate. The shell-model calculations predict the 3^- state about 300 keV below, at 3032 keV, though this could be a systematic underestimation as for ^{68}Ni the calculated 3^- state, at 2868 keV, lies about 400 keV below the experimental one, at 3302 keV [8,49,54].

The $\log ft$ values of 5.30(15), 5.51(2), and 5.80(4) measured to the $(0-2)^+$ states at 4135, 4478, and 5105 keV indicate that a significant part of the β strength from the low-spin isomer is shifted to levels between 4 and 5 MeV. This is at variance with the β decay of the analogous states in lighter Co isotopes, which undergo stronger β transitions to the (2_1^+) and (2_2^+) levels [8,11,38]. All these experimental findings point to a change in the wave function of the low-spin isomer of odd-odd Co isotopes at mass $A = 72$. As previously anticipated, a $J^\pi = (0^+)$ or (1^+) assignment is tentatively proposed based on the reduced population of the (2_1^+) and (2_2^+) candidates and the enhanced feeding to the 0^+ ground state as compared to the neighboring ^{70}Co [11]. Under such an assumption, the low- J initial level is expected to feed the 1^+ state in ^{72}Ni . The excitation energy predicted by the shell-model calculations, at 5159 keV, compares well with the location of the 5105-keV experimental level. The nonobservance of the direct transition to the ground state might be ascribed to the limited γ efficiency of the EURICA array for high-energy γ rays. It should be noted, yet, that the $J^\pi = (0^+)$ or (1^+) tentative assignment for the low- J isomer suggest the coexistence of spherical ($J^\pi = 6^-$ or 7^-) and deformed ($J^\pi = 0^+$ or 1^+) shapes in ^{72}Co , and, hence, a deformed $J^\pi = (0^+, 1^+)$ state would preferentially decay to deformed 0^+-2^+ levels rather than to spherical ones. As well, the population of the 0^+ prolate bandhead predicted at low excitation energy in Ref. [2] would be favored. The nonobservation of a good experimental counterpart in the present work does not necessarily imply the absence of a low-lying intruder deformed 0^+ level, but might be attributable to the fact that it does not decay by γ emission.

Note that part of the large β branching ratio to the ground state, $I_\beta \leq 42(13)\%$, might result from the nonobservation of such an excited 0^+ level.

VI. SUMMARY AND CONCLUSIONS

The present work provides a significantly improved review on the low-lying energy structure of ^{72}Ni . This nucleus has been investigated in a β -decay experiment performed at the RIBF facility of the RIKEN Nishina Center, in Japan. The high intensities reached by the RIBF accelerator system, together with the high performance of the state-of-the-art BigRIPS and EURICA setups have allowed for a detailed study of the decay $^{72}\text{Co} \rightarrow ^{72}\text{Ni}$ and have provided first experimental information on the decay sequences $^{72}\text{Fe} \rightarrow ^{72}\text{Co} \rightarrow ^{72}\text{Ni}$ and $^{73}\text{Co} \rightarrow ^{72}\text{Ni}$. As a result, a wealthy set of new levels has been observed and compared to shell-model calculations in the reduced neutron fpg valence space. Candidates for the (4_2^+) , (6_2^+) , and (8_1^+) levels related to seniorities $\nu = 2$ and $\nu = 4$ have been presented, and a general good agreement between theory and experiment (excepting the 2455-keV state) has been found.

The existence of the low-spin β -decaying isomer previously observed in lighter odd-odd neutron-rich Co isotopes has been confirmed in ^{72}Co . The quasinull β feeding to the levels tentatively assigned to $J^\pi = (2^+)$ and the prominent population of the ground state can be considered as experimental fingerprints for a change in the nature of the isomer, with a proposed $J^\pi = (0^+)$ or (1^+) in ^{72}Co as compared to the $J^\pi = (3^+)$, (1^\pm) , and (2^-) assignments suggested in previous works for ^{68}Ni and ^{70}Ni . The nonobservation of a clear (0^+) deformed candidate at the energy predicted by Tsunoda *et al.* [2] following the decay of the isomer has been discussed, concluding that further experimental efforts will have to be focused on the search of a possible low-lying (0^+) level decaying mainly by an $E0$ transition or electron-positron pair production. This will definitely confirm or discard the existence of deformed structures at low excitation energies in ^{72}Ni .

ACKNOWLEDGMENTS

The excellent work of the RIKEN accelerator staff for providing a stable and high-intensity ^{238}U beam is acknowledged. We acknowledge the EUROBALL Owners Committee for the loan of germanium detectors and the PreSpec Collaboration for the readout electronics of the cluster detectors. Part of the WAS3ABi was supported by the Rare Isotope Science Project, which is funded by the Ministry of Science, ICT and Future Planning (MSIP) and National Research Foundation (NRF) of Korea. This work is cofinanced by the European Union and the European Social Fund. Support from Italian Programmi di Ricerca Scientifica di Rilevante Interesse Nazionale (PRIN) Grant No. 2001024324_01302, the NuPNET-ERANET within the NuPNET GANAS project under Grant Agreement No. 202914, and the European Union within the 7th Framework Program FP7/2007-2013 under Grant Agreement No. 262010 ENSAR-INDESYS is acknowledged. This work was also financed by the Spanish Ministerio de Ciencia e

Innovación under Contracts No. FPA2009-13377-C02 and No. FPA2011-29854-C04, the Hungarian Research Fund OTKA Contract No. K100835 and No. K106035, the European

Commission through the Marie Curie Actions Contract No. PIEFGA-2001-30096, and by the Japanese JSPS KAKENHI Grants No. 24740188 and No. 25247045.

- [1] T. Otsuka, T. Suzuki, R. Fujimoto, H. Grawe, and Y. Akaishi, *Phys. Rev. Lett.* **95**, 232502 (2005).
- [2] Y. Tsunoda, T. Otsuka, N. Shimizu, M. Honma, and Y. Utsuno, *Phys. Rev. C* **89**, 031301 (2014).
- [3] L. Coraggio, A. Covello, A. Gargano, and N. Itaco, *Phys. Rev. C* **89**, 024319 (2014).
- [4] K. Kaneko, T. Mizusaki, Y. Sun, and S. Tazaki, *Phys. Rev. C* **92**, 044331 (2015).
- [5] S. M. Lenzi, F. Nowacki, A. Poves, and K. Sieja, *Phys. Rev. C* **82**, 054301 (2010).
- [6] F. Recchia, C. J. Chiara, R. V. F. Janssens, D. Weisshaar, A. Gade, W. B. Walters, M. Albers, M. Alcorta, V. M. Bader, T. Baugher *et al.*, *Phys. Rev. C* **88**, 041302 (2013).
- [7] S. Suchyta, S. N. Liddick, Y. Tsunoda, T. Otsuka, M. B. Bennett, A. Chemey, M. Honma, N. Larson, C. J. Prokop, S. J. Quinn *et al.*, *Phys. Rev. C* **89**, 021301 (2014).
- [8] F. Flavigny, D. Pauwels, D. Radulov, I. J. Darby, H. De Witte, J. Diriken, D. V. Fedorov, V. N. Fedosseev, L. M. Fraile, M. Huyse *et al.*, *Phys. Rev. C* **91**, 034310 (2015).
- [9] C. J. Chiara, D. Weisshaar, R. V. F. Janssens, Y. Tsunoda, T. Otsuka, J. L. Harker, W. B. Walters, F. Recchia, M. Albers, M. Alcorta *et al.*, *Phys. Rev. C* **91**, 044309 (2015).
- [10] C. J. Prokop, B. P. Crider, S. N. Liddick, A. D. Ayangeakaa, M. P. Carpenter, J. J. Carroll, J. Chen, C. J. Chiara, H. M. David, A. C. Dombos *et al.*, *Phys. Rev. C* **92**, 061302 (2015).
- [11] A. I. Morales *et al.* (unpublished).
- [12] M. Sawicka, R. Grzywacz, I. Matea, H. Grawe, M. Pfützner, J. M. Daugas, M. Lewitowicz, D. L. Balabanski, F. Becker, G. Béliet *et al.*, *Phys. Rev. C* **68**, 044304 (2003).
- [13] C. Mazzocchi, R. Grzywacz, J. Batchelder, C. Bingham, D. Fong, J. Hamilton, J. Hwang, M. Karny, W. Krolas, S. Liddick *et al.*, *Phys. Lett. B* **622**, 45 (2005).
- [14] I. Talmi, *Simple Models of Complex Nuclei. The Shell Model and Interacting Boson Model* (Harwood, Academic, Chur, Switzerland, 1993).
- [15] R. Casten, *Nuclear Structure from a Simple Perspective* (Oxford University Press, New York, 2000).
- [16] R. Grzywacz, R. Béraud, C. Borcea, A. Emsallem, M. Glogowski, H. Grawe, D. Guillemaud-Mueller, M. Hjorth-Jensen, M. Houry, M. Lewitowicz *et al.*, *Phys. Rev. Lett.* **81**, 766 (1998).
- [17] M. Görska, M. Lipoglavšek, H. Grawe, J. Nyberg, A. Atac, A. Axelsson, R. Bark, J. Blomqvist, J. Cederkäll, B. Cederwall *et al.*, *Phys. Rev. Lett.* **79**, 2415 (1997).
- [18] A. Jungclaus, L. Cáceres, M. Görska, M. Pfützner, S. Pietri, E. Werner-Malento, H. Grawe, K. Langanke, G. Martínez-Pinedo, F. Nowacki *et al.*, *Phys. Rev. Lett.* **99**, 132501 (2007).
- [19] H. Watanabe, G. Lorusso, S. Nishimura, Z. Y. Xu, T. Sumikama, P.-A. Söderström, P. Doornenbal, F. Browne, G. Gey, H. S. Jung *et al.*, *Phys. Rev. Lett.* **111**, 152501 (2013).
- [20] A. Gottardo, J. J. Valiente-Dobón, G. Benzoni, R. Nicolini, A. Gadea, S. Lunardi, P. Boutachkov, A. M. Bruce, M. Görska, J. Grebosz *et al.*, *Phys. Rev. Lett.* **109**, 162502 (2012).
- [21] P.-A. Söderström, S. Nishimura, Z. Y. Xu, K. Sieja, V. Werner, P. Doornenbal, G. Lorusso, F. Browne, G. Gey, H. S. Jung *et al.*, *Phys. Rev. C* **92**, 051305 (2015).
- [22] H. Grawe, M. Görska, C. Fahlander, M. Palacz, F. Nowacki, E. Caurier, J. Daugas, M. Lewitowicz, M. Sawicka, R. Grzywacz *et al.*, *Nucl. Phys. A* **704**, 211 (2002).
- [23] A. F. Lisetskiy, B. A. Brown, M. Horoi, and H. Grawe, *Phys. Rev. C* **70**, 044314 (2004).
- [24] P. V. Isacker, *Int. J. Mod. Phys. E* **20**, 191 (2011).
- [25] C. J. Chiara, W. B. Walters, I. Stefanescu, M. Alcorta, M. P. Carpenter, B. Fornal, G. Gürdal, C. R. Hoffman, R. V. F. Janssens, B. P. Kay *et al.*, *Phys. Rev. C* **84**, 037304 (2011).
- [26] M. M. Rajabali, R. Grzywacz, S. N. Liddick, C. Mazzocchi, J. C. Batchelder, T. Baumann, C. R. Bingham, I. G. Darby, T. N. Ginter, S. V. Ilyushkin *et al.*, *J. Phys. G: Nucl. Part. Phys.* **41**, 115104 (2014).
- [27] S. Nishimura, *Prog. Theor. Exp. Phys.* **03C006** (2012).
- [28] N. Fukuda, T. Kubo, T. Ohnishi, N. Inabe, H. Takeda, D. Kameda, and H. Suzuki, *Nucl. Instrum. Methods B* **317**, 323 (2013).
- [29] Y. Mizoi *et al.*, RIKEN Accel. Prog. Rep. **38**, 297 (2005).
- [30] P.-A. Söderström, S. Nishimura, P. Doornenbal, G. Lorusso, T. Sumikama, H. Watanabe, Z. Xu, H. Baba, F. Browne, S. Go *et al.*, *Nuclear Instr. and Methods B* **317**, 649 (2012).
- [31] J. Eberth, P. V. Brentano, W. Teichert, H. Thomas, A. Werth, R. Lieder, H. Jäger, H. Kämmerling, D. Kutchin, K. Maier *et al.*, *Prog. Part. Nucl. Phys.* **28**, 495 (1992).
- [32] Z. Patel *et al.*, RIKEN Accelerator Progress Report, 2014.
- [33] Z. Xu, Ph.D. thesis, University of Tokyo, 2014.
- [34] J. Taprogge, A. Jungclaus, H. Grawe, S. Nishimura, P. Doornenbal, G. Lorusso, G. S. Simpson, P.-A. Söderström, T. Sumikama, Z. Y. Xu *et al.*, *Phys. Rev. C* **91**, 054324 (2015).
- [35] A. I. Morales, G. Benzoni, H. Watanabe, D. Sohler, E. Sahin, G. de Angelis, S. Nishimura, G. Lorusso, T. Sumikama, P. Doornenbal *et al.*, in *Exotic Nuclei* (World Scientific, Singapore, 2015), Chap. 45, p. 429.
- [36] F. Browne *et al.*, *Phys. Lett. B* **750**, 448 (2015).
- [37] M. Wang, G. Audi, A. Wapstra, F. Kondev, M. MacCormick, X. Xu, and B. Pfeiffer, *Chin. Phys. C* **36**, 1603 (2012).
- [38] W. F. Mueller, B. Bruyneel, S. Franchoo, M. Huyse, J. Kurpeta, K. Kruglov, Y. Kudryavtsev, N. V. S. V. Prasad, R. Raabe, I. Reusen *et al.*, *Phys. Rev. C* **61**, 054308 (2000).
- [39] U. Bosch, W.-D. Schmidt-Ott, E. Runte, P. Tidemand-Petersson, P. Koschel, F. Meissner, R. Kirchner, O. Klepper, E. Roeckl, K. Rykaczewski *et al.*, *Nucl. Phys. A* **477**, 89 (1988).
- [40] W. F. Mueller, B. Bruyneel, S. Franchoo, H. Grawe, M. Huyse, U. Köster, K.-L. Kratz, K. Kruglov, Y. Kudryavtsev, B. Pfeiffer *et al.*, *Phys. Rev. Lett.* **83**, 3613 (1999).
- [41] M. Sawicka, I. Matea, H. Grawe, R. Grzywacz, M. Pfützner, M. Lewitowicz, J. Daugas, B. Brown, A. Lisetskiy, F. Becker *et al.*, *Eur. Phys. J. A* **22**, 455 (2004).
- [42] I. Stefanescu, D. Pauwels, N. Bree, T. E. Cocolios, J. Diriken, S. Franchoo, M. Huyse, O. Ivanov, Y. Kudryavtsev, N. Patronis *et al.*, *Phys. Rev. C* **79**, 044325 (2009).

- [43] M. M. Rajabali, R. Grzywacz, S. N. Liddick, C. Mazzocchi, J. C. Batchelder, T. Baumann, C. R. Bingham, I. G. Darby, T. N. Ginter, S. V. Ilyushkin *et al.*, *Phys. Rev. C* **85**, 034326 (2012).
- [44] D. Pauwels, O. Ivanov, N. Bree, J. Büscher, T. E. Cocolios, J. Gentens, M. Huyse, A. Korgul, Y. Kudryavtsev, R. Raabe *et al.*, *Phys. Rev. C* **78**, 041307 (2008).
- [45] S. N. Liddick, B. Abromeit, A. Ayres, A. Bey, C. R. Bingham, M. Bolla, L. Cartegni, H. L. Crawford, I. G. Darby, R. Grzywacz *et al.*, *Phys. Rev. C* **85**, 014328 (2012).
- [46] J. Hardy, L. Carraz, B. Jonson, and P. Hansen, *Phys. Lett. B* **71**, 307 (1977).
- [47] ENSDF, <http://www.nndc.bnl.gov/ensdf/>
- [48] Z. Y. Xu, S. Nishimura, G. Lorusso, F. Browne, P. Doornenbal, G. Gey, H.-S. Jung, Z. Li, M. Niikura, P.-A. Söderström *et al.*, *Phys. Rev. Lett.* **113**, 032505 (2014).
- [49] R. Broda, T. Pawlat, W. Królas, R. V. F. Janssens, S. Zhu, W. B. Walters, B. Fornal, C. J. Chiara, M. P. Carpenter, N. Hoteling *et al.*, *Phys. Rev. C* **86**, 064312 (2012).
- [50] T. E. Milliman, J. P. Connelly, J. H. Heisenberg, F. W. Hersman, J. E. Wise, and C. N. Papanicolas, *Phys. Rev. C* **41**, 2586 (1990).
- [51] P. Beuzit, J. Delaunay, and J. Fouan, *Nucl. Phys. A* **128**, 594 (1969).
- [52] E. Caurier, G. Martínez-Pinedo, F. Nowacki, A. Poves, and A. P. Zuker, *Rev. Mod. Phys.* **77**, 427 (2005).
- [53] G. Benzoni, A. I. Morales, H. Watanabe, S. Nishimura, L. Coraggio, N. Itaco, A. Gargano, F. Browne, R. Daido, P. Doornenbal *et al.*, *Phys. Lett. B* **751**, 107 (2015).
- [54] C. J. Chiara, R. Broda, W. B. Walters, R. V. F. Janssens, M. Albers, M. Alcorta, P. F. Bertone, M. P. Carpenter, C. R. Hoffman, T. Lauritsen *et al.*, *Phys. Rev. C* **86**, 041304 (2012).